

Received December 28, 2019, accepted January 15, 2020, date of publication February 10, 2020, date of current version February 18, 2020.

Digital Object Identifier 10.1109/ACCESS.2020.2973000

Generic Deep Learning-Based Linear Detectors for MIMO Systems Over Correlated Noise Environments

KE HE¹, ZIZHI WANG¹, WEI HUANG¹, DAN DENG², JUNJUAN XIA¹, AND LISENG FAN¹

¹School of Computer Science and Cyber Engineering, Guangzhou University, Guangzhou 510006, China

²School of Information Engineering, Guangzhou Panyu Polytechnic, Guangzhou 511483, China

Corresponding authors: Junjuan Xia (xiajunjuan@gzhu.edu.cn) and Liseng Fan (lsfan2019@126.com)

This work was supported in part by the Graduate Innovative Research Grant Program of Guangzhou University under Grant 2019GDJC-M18, in part by the Natural Science Foundation of Guangdong Province under Grant 2018A030313736, in part by the Scientific Research Project of Education Department of Guangdong, China, under Grant 2017GKTSCX045, and in part by the Project of Technology Development Foundation of Guangdong under Grant 706049150203.

ABSTRACT To support the development and application of the fifth-generation (5G) communication and internet of things (IoT) networks, high data-rate wireless transmission is required. To meet the demand of high data-rate, multiple antennas are equipped at the transmitter and receiver, forming multiple-input multiple-output (MIMO) systems. A big challenge of MIMO is the detector design in correlated noise environments, which should achieve a fine performance with moderate computational complexity. To this end, we employ an iterative framework of a deep convolutional neural network (DCNN) and a linear detector for MIMO systems over correlated noise environments. In this framework, the linear detector can be zero-forcing (ZF), minimum mean square error (MMSE), ZF with successive interference cancellation (ZF-SIC), or MMSE-SIC, which produces an initial estimate of transmitted signals. The DCNN is used to capture the local correlation among noise, and it can produce a more accurate estimate of transmitted signals. Simulation results are finally provided to show that the proposed detector can outperform the conventional linear detectors substantially through capturing the local correlation characteristics among noise.

INDEX TERMS Deep learning, MIMO, correlated noise.

I. INTRODUCTION

With the deployment and development of the fifth-generation (5G) wireless communication systems [1]–[3], there is an explosively increasing progress in the data rate for wireless transmission [4]–[6]. To meet this requirement, many new techniques have been proposed to enhance the transmission quality and optimize the system resource management. Among these techniques, relaying technique is an effective one, which can help increase the coverage area and improve the transmission quality, without requiring additional transmit power [7]–[9]. There are two fundamental relaying protocols, such as amplify-and-forward (AF) and decode-and-forward (DF). Besides these two relaying protocols, there are some other relaying protocols in the literature. The usage of relaying can help increase transmission security

in the wireless networks, which also receives much attention from the academia and industry [10]–[12].

Besides the relaying technique, multiple antenna technique is an effective solution to meet demand, and it has been proven that the data rate can be linearly proportional to the number of antenna in multiple-input multiple-output (MIMO) systems [13]–[16]. A high challenge in MIMO systems is that how to effectively detect the transmitted signals at the receiver side [17]–[19]. In uncorrelated noise environments, the optimal MIMO detector is the maximum likelihood detector (MLD), which has the exponentially increasing computational complexity with respect to the number of transmit antenna and modulation size [20], [21]. To reduce the computational complexity, some linear detectors have been proposed for the MIMO systems, such as zero-forcing (ZF) and minimum mean square error (MMSE) detectors. The main drawbacks of the linear detectors is the noise enhancement, which can be relieved by the successive interference cancellation (SIC) technique to some extent.

The associate editor coordinating the review of this manuscript and approving it for publication was Guan Gui¹.

The above detectors can work for MIMO systems in uncorrelated noise environments. However, in practice, the noise in MIMO systems may be correlated, due to many practical reasons [22]–[24]. For example, the noise may be correlated in the time domain when it continues on two or more time symbols; the noise may be correlated in the frequency domain when the channel estimation and synchronization are not ideal in the orthogonal frequency division multiplexing (OFDM) systems. In correlated noise environments, the correlation among different symbols can be exploited to improve the detection performance. In theory, the optimal detector in correlated noise environments is the maximum likelihood sequential detector (MLSD). There are two main limitations of MLSD in practice. The first limitation is the huge computational complexity, which exponentially increases with respect to the number of symbols in a transmission packet, number of transmit antenna, and the modulation size. Another limitation is that it requires the knowledge about the distributions of correlated noise among a packet, which is very difficult or even impossible to estimate in practice, especially when the correlation is time-varying.

Inspired by the recent progress on the intelligent data-driven networks applied in wireless communications [25]–[27], we turn to study the deep learning based detection for the MIMO systems under correlated noise environments. Deep learning is a data-driven method which can efficiently exploit the huge amount of wireless data for communication systems [28]–[30]. In particular, we apply an iterative framework of a deep convolutional neural network (DCNN) and a linear detector, where the DCNN is utilized to capture the local correlation among noise in different symbols [31]. The linear detector can be ZF, MMSE, Zf-SIC, or MMSE-SIC, which requires very limited computational complexity to implement. The linear detector produces an initial estimate of the transmitted signals, while the DCNN can produce a more accurate estimate of transmitted signals by exploiting the local correlation among noise. This iterative process continues, and it can help improve the detection performance for the linear detection. Finally, we provide some simulation results to validate the proposed studies.

The organization of this paper is given as follows. After the introduction in this section, we will discuss the system model of MIMO in Sec. II, and then introduce the linear detectors in Sec. III. After that, we will describe the iterative framework of DCNN and linear detectors in Sec. IV. Sec. V will present the simulation results and conclusions are finally made in Sec. VI.

II. SYSTEM MODEL

In this paper, we consider an $M \times M$ MIMO system, where there are M antennas at the transmitter and receiver. The MIMO channel follows time-varying Rayleigh fading, and it remains unchanged within the same transmission packet. For the n -th symbol ($1 \leq n \leq N$), the received signal at the m_1 -th

receiver is given by

$$y_{m_1}(n) = \sum_{m_2=1}^M h_{m_2, m_1} s_{m_2}(n) + w_{m_1}(n), \quad (1)$$

where $s_{m_2}(n)$ is the transmitted signal at the m_2 -th transmit antenna, following some specific modulation scheme such as binary phase shift keying (BPSK) or quadrature phase shift keying (QPSK), and $w_{m_1}(n) \sim \mathcal{CN}(0, \sigma^2)$ is the additive white Gaussian noise (AWGN) at the receiver, where the details about the noise can be found in the literature [32], [33]. Notation $h_{m_2, m_1} \sim \mathcal{CN}(0, 1)$ represents the channel coefficient between the m_2 -th transmit antenna and m_1 -th receive antenna. By using the vector and matrix forms, we can rewrite (1) as

$$\mathbf{y}(n) = \mathbf{H}\mathbf{s}(n) + \mathbf{w}(n). \quad (2)$$

When the noise $\mathbf{w}(n)$ is independent among different symbols, the optimal detector for MIMO systems is the maximum likelihood detector (MLD), whose computational complexity exponentially increases with M and the modulation size. On the contrary, when the noise is correlated among different symbols, the optimal detector for MIMO systems is the maximum likelihood sequential detector (MLSD), whose computational complexity exponentially increases with M, N and the modulation size. This motivates us to study the linear detector for MIMO systems, which will be detailed in the next section.

III. LINEAR DETECTORS

In this section, we will describe four linear detectors, i.e., ZF, MMSE, ZF-SIC and MMSE-SIC, for the MIMO systems.

A. ZF DETECTOR

The ZF detector performs the detection by removing the spatial correlation among antennas in a forcing way, i.e.,

$$\mathbf{y}_{ZF}(n) = (\mathbf{H}^H \mathbf{H})^{-1} \mathbf{H}^H \mathbf{y}(n), \quad (3)$$

where the subscript H denotes the operation of conjugate transpose. Then, from each element in $\mathbf{y}_{ZF}(n)$, the component-wise detection is used. In this way, the ZF detector is completed. The ZF detection is quite simple to implement in practice, at the cost of severe noise enhancement in the detection. Specifically, the noise varies from $\mathbf{w}(n)$ to $(\mathbf{H}^H \mathbf{H})^{-1} \mathbf{H}^H \mathbf{w}(n)$, and the noise variance matrix changes from $\sigma^2 \mathbf{I}$ to $(\mathbf{H}^H \mathbf{H})^{-1} \sigma^2$. When there exists a very small eigenvalue in $\mathbf{H}^H \mathbf{H}$, the noise will be severely enhanced in the detection, which limits the detection performance substantially.

B. MMSE DETECTOR

To implement the linear detector and meanwhile suppress the severe noise enhancement in ZF detector, the MMSE detection can be used, which is given by

$$\mathbf{y}_{MMSE}(n) = (\mathbf{H}^H \mathbf{H} + \sigma^2 \mathbf{I})^{-1} \mathbf{H}^H \mathbf{y}(n). \quad (4)$$

Then, from each element in $\mathbf{y}_{MMSE}(n)$, the component-wise detection is used. In this way, the MMSE detection is completed. Note that the noise component in MMSE detector changes from $\mathbf{w}(n)$ to $(\mathbf{H}^H \mathbf{H} + \sigma^2 \mathbf{I})^{-1} \mathbf{H}^H \mathbf{w}(n)$. Accordingly, the noise covariance matrix enlarges from $\sigma^2 \mathbf{I}$ to $(\mathbf{H}^H \mathbf{H} + \sigma^2 \mathbf{I})^{-1} \mathbf{H}^H \mathbf{H} (\mathbf{H}^H \mathbf{H} + \sigma^2 \mathbf{I})^{-1} \sigma^2$. By comparing with the noise covariance in ZF detector, we can find that the MMSE detector can outperform the ZF detector through suppressing the noise enhancement to some extent.

C. ZF-SIC DETECTOR

Another way to suppress the effect of noise enhancement in ZF detector is to introduce the operation of SIC [34]–[36]. In ZF-SIC, the detection sequence of transmitted signals is firstly determined according to the diagonal element of matrix $(\mathbf{H}^H \mathbf{H})^{-1}$, given by

$$(\mathbf{H}^H \mathbf{H})_{m,m}^{-1}. \tag{5}$$

According to the minimum value of $(\mathbf{H}^H \mathbf{H})_{m,m}^{-1}$, the system chooses the first transmitted signal to be detected, whose index is denoted by m_1 . Then, the m_1 -th transmitted signal is firstly estimated from $\mathbf{y}_{ZF}(n)$, given by $\hat{s}_{m_1}(n)$. After that, the received signal $\mathbf{y}(n)$ is updated as

$$\mathbf{y}_1(n) = \mathbf{y}(n) - \mathbf{h}_{m_1} \hat{s}_{m_1}(n). \tag{6}$$

Accordingly, the channel matrix is updated from \mathbf{H} to \mathbf{H}_1 by removing the m_1 -th column. Then, the ZF detected signal is updated as

$$\mathbf{y}_{1,ZF}(n) = (\mathbf{H}_1^H \mathbf{H}_1)^{-1} \mathbf{H}_1^H \mathbf{y}_1(n). \tag{7}$$

From $\mathbf{y}_{1,ZF}(n)$, the m_2 -th transmitted signal with the minimum value of $(\mathbf{H}_1^H \mathbf{H}_1)_{m,m}^{-1}$ is detected, and its estimate is given by $s_{m_2}(n)$. This process continues until the last transmitted signal $s_{m_M}(n)$ is detected. In this way, the ZF-SIC procedure is completed.

D. MMSE-SIC DETECTOR

Similar to ZF-SIC, the SIC can be also incorporated into MMSE to enhance its detection performance. In MMSE-SIC, the detection sequence of transmitted signals is firstly determined according to the diagonal element of matrix $(\mathbf{H}^H \mathbf{H} + \sigma^2 \mathbf{I})^{-1}$, given by

$$(\mathbf{H}^H \mathbf{H} + \sigma^2 \mathbf{I})_{m,m}^{-1}. \tag{8}$$

According to the minimum value of $(\mathbf{H}^H \mathbf{H} + \sigma^2 \mathbf{I})_{m,m}^{-1}$, the system chooses the first transmitted signal to be detected, whose index is denoted by m_1 . Then, the m_1 -th transmitted signal is firstly estimated from $\mathbf{y}_{MMSE}(n)$, given by $\hat{s}_{m_1}(n)$. After that, the received signal $\mathbf{y}(n)$ is updated as

$$\mathbf{y}_1(n) = \mathbf{y}(n) - \mathbf{h}_{m_1} \hat{s}_{m_1}(n). \tag{9}$$

Accordingly, the channel matrix is updated from \mathbf{H} to \mathbf{H}_1 by removing the m_1 -th column. Then, the MMSE detected signal is updated as

$$\mathbf{y}_{1,MMSE}(n) = (\mathbf{H}_1^H \mathbf{H}_1 + \sigma^2 \mathbf{I})^{-1} \mathbf{H}_1^H \mathbf{y}_1(n). \tag{10}$$

From $\mathbf{y}_{1,MMSE}(n)$, the m_2 -th transmitted signal associated with the minimum value of $(\mathbf{H}_1^H \mathbf{H}_1 + \sigma^2 \mathbf{I})_{m,m}^{-1}$ is detected, and its estimate is given by $s_{m_2}(n)$. This process continues until the last transmitted signal $s_{m_M}(n)$ is detected. In this way, the MMSE-SIC procedure is completed.

IV. PROPOSED GENERIC DEEP LEARNING BASED ITERATIVE DETECTION FRAMEWORK

Inspired by the recent advances in deep learning technologies and in order to improve the performance of the linear detectors in the presence of correlated noise, we propose a generic deep learning based iterative detection framework, which contains a linear detector and a deep convolutional neural network (DCNN) at the receiver. We will introduce the system structure as well as the DCNN in the next two subsections. Computational complexity analysis of the proposed iterative framework is presented at the last subsection.

A. A GENERIC ITERATIVE FRAMEWORK FOR LINEAR DETECTORS

As shown in Fig. 1, a linear detector and a DCNN are jointly used. The detector can be any kind of linear detectors, such as ZF, MMSE, ZF-SIC or MMSE-ISC. The detection workflow iteratively passes through the linear detector and DCNN in K iterations and the finally estimated signal is generated at the last iteration.

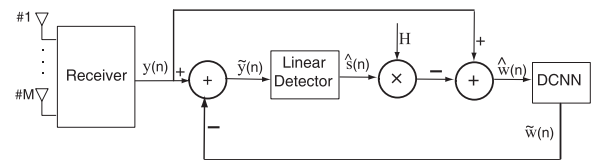


FIGURE 1. Structure of the generic deep learning based iterative detection framework.

Basically, at each iteration, the linear detector firstly estimates the signal from the received signal and channel matrix, denoted by $\hat{\mathbf{s}}$. After that, we can estimate the noise as

$$\hat{\mathbf{w}}(n) = \mathbf{y}(n) - \mathbf{H}\hat{\mathbf{s}}(n). \tag{11}$$

Inspired by the successful application of residual learning for image denoising [37] and notice that if the detection result $\hat{\mathbf{s}}$ is not correct, the estimate of noise $\hat{\mathbf{w}}$ is not correct as well. We employ the DCNN to learn the latent correlation of $\hat{\mathbf{w}}$ and recover a more accurate estimation of the noise, which is given by

$$\tilde{\mathbf{w}}(n) = \mathbb{F}(\hat{\mathbf{w}}(n)), \tag{12}$$

where $\mathbb{F}(\cdot)$ represents an nonlinear transformation function parameterized by the DCNN. Thus, we can cancel the influence of correlated noises by

$$\tilde{\mathbf{y}}(n) = \mathbf{y}(n) - \tilde{\mathbf{s}}(n) \tag{13}$$

$$= \mathbf{H}\hat{\mathbf{s}}(n) + \mathbf{w}(n) - \tilde{\mathbf{w}}(n) \tag{14}$$

$$\triangleq \mathbf{H}\hat{\mathbf{s}}(n) + \mathbf{z}(n), \tag{15}$$

where $\mathbf{z}(n) = \mathbf{w}(n) - \tilde{\mathbf{w}}(n)$ represents the effective residual noise. Note that if the estimation of noise produced by the DCNN is more accurate compared with the prior linear detector, the effective SNR is increased for $\tilde{\mathbf{y}}(n)$. Hence, we can feed back the effective signal $\tilde{\mathbf{y}}(n)$ to the linear detector to improve the detection performance at the incoming iterations.

B. DEEP CONVOLUTIONAL NEURAL NETWORK

Fig. 2 shows the DCNN structure of the proposed generic iterative detection framework. Generally, the DCNN contains L convolutional layers and each layer contains F_l filters, where $l \in [1, 2, \dots, L]$. For each filter denoted by $filter_{(l,j)}$ ($j \in [1, 2, \dots, F_l]$) at the l -th layer, it will firstly perform zero-padding operation for the input data with the purpose of keeping the same length after convolution operation. After that, it will perform 1-D convolution on the padded data with kernel size of R_l to generate a corresponding feature map with rectified linear unit (ReLU) [38] activation function.

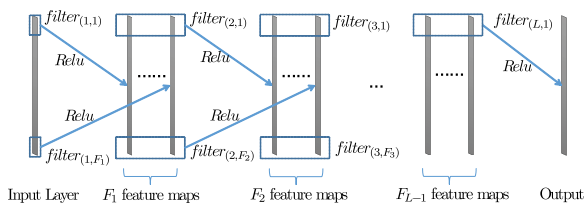


FIGURE 2. Structure of deep convolutional neural network.

Specifically, the first layer is the input layer and the last layer is the output layer. The rest layers are the hidden layers. For the first layer, it receives $\hat{\mathbf{w}}$ and produces F_1 feature maps for the second layer. For any hidden layer, it receives F_{l-1} feature maps from the prior layer and generates F_l feature maps for the posterior layer. For the last layer, it has only one filter, because we have to maintain the same spatial dimension as the input data. For convenience, we denote the DCNN structure as

$$\{L; R_1, R_2, \dots, R_L; F_1, F_2, \dots, F_L\}. \quad (16)$$

As we have discussed earlier, the training objective of DCNN is to generate a more accurate estimation of noise from $\hat{\mathbf{w}}$ as much as possible. This is equivalent to minimize the effective residual noise \mathbf{z} . In pursuing this objective, we employ the mini-batch stochastic gradient descending [39] and the L_2 -norm loss function to train the learnable variables in the neural networks, so that we can obtain the loss value for every mini-batch size of N time slots as

$$Loss = \frac{1}{N} \sum_{n=1}^N \|\mathbf{w} - \tilde{\mathbf{w}}\|^2 \quad (17)$$

$$= \frac{1}{N} \sum_{n=1}^N \|\mathbf{z}\|^2. \quad (18)$$

C. COMPUTATIONAL COMPLEXITY ANALYSIS

For any detection algorithm, its computational complexity is always an issue we have to face. In this subsection, we analyze the required computational complexity caused by K iterations. The consumption of computation at each iteration in the proposed generic iterative detection framework is consisting of two parts: the computational complexities of the linear detector as well as the DCNN.

For linear detectors, we denoted the required computational complexity as \mathcal{O}_D , where it is of $\mathcal{O}(M)$ for the linear detectors. For the DCNN, the computational complexity is given by [40]:

$$\mathcal{O} \left(\sum_{l=1}^L (F_{l-1} R_l M F_l) \right). \quad (19)$$

Therefore, the total computational complexity of the proposed framework is given by summing up these two parts for K iterations:

$$\mathcal{O} \left((K + 1) \mathcal{O}_D + K \sum_{l=1}^L (F_{l-1} R_l M F_l) \right). \quad (20)$$

From the above expression, we can see that the computational complexity of the generic iterative detection framework increases almost linearly with the number of iterations, which indicates that the extra computational complexity caused by the iterative framework is computationally tractable and acceptable.

V. SIMULATION RESULTS AND DISCUSSIONS

In this section, we present some simulation results in order to verify the effectiveness of the proposed generic iterative detection framework. The binary phase shift keying (BPSK) modulation is adopted at the transmitter, and both the transmitter and receiver contain $M = 4$ antennas. In addition, the channel matrix is time-varying and we apply a typical model, namely the Jakes model [41], to generate the channel matrix with the normalized Doppler frequency f_d setting to 0.1.

Specifically, we employ a typical temporal correlation model to generate the correlated noise [41], which is described by:

$$\mathbf{w}(n + 1) = \sqrt{\rho} \mathbf{w}(n) + \sqrt{1 - \rho} \mathbf{u}(n + 1), \quad (21)$$

where $\mathbf{u}(n + 1) \sim \mathcal{CN}(0, \sigma^2 \mathbf{I})$ is an additive noisy term independent of $\mathbf{w}(n)$, and $0 \leq \rho \leq 1$ is the correlation coefficient. Specifically, $\rho = 0$ represents the uncorrelated scenario, while $\rho = 1$ represents the completely correlated scenario, respectively.

Moreover, with respect to the structure of DCNN, we use four convolutional layers, so that $L = 4$. The number of filters and filter sizes at each layer are set to $\{64, 32, 16, 1\}$ and $\{9, 3, 3, 15\}$, respectively. Therefore, we summarize the DCNN structure as $\{4; 9, 3, 3, 15; 64, 32, 16, 1\}$. The maximum number of iterations between the linear detector and the DCNN K is set to 3.

Regarding the data set, we set the mini-batch size to $N = 720$ time slots, so that it is only consisting of 720 time slots of the received signals \mathbf{y} , the channel matrix \mathbf{H} and the correlated noises \mathbf{w} suffered from the transmission for every data batch. To train the learnable variables inside the DCNN filters, we generate 10,000 batches for training set. To valid the generalization ability during the training process and test the performance after finishing the training, the valid set and test set both contain 1,000 batches. The simulation settings of important parameters are summarized in Table. 1 for convenience.

TABLE 1. summary of simulation settings.

Parameter	Value
K	3
L	4
$\{R_1, R_2, \dots, R_L\}$	$\{36, 3, 3, 36\}$
$\{F_1, F_2, \dots, F_L\}$	$\{32, 16, 8, 1\}$
M	4
f_d	0.1
ρ	From 0 to 0.9 (0.1 each step)
SNR	From 0 dB to 20 dB (2 dB each step)
N	720
Total Training batches	10,000
Total valid batches	1,000
Total test batches	1,000

Fig. 3 shows that the effect of correlation coefficient ρ on the BER performance for the ZF detector and the ZF based iterative detector (ZF-DCNN) detector, where the signal-to-noise ratio(SNR) is set to 30 dB. The correlation coefficient ρ varies from 0 to 0.9, where $\rho = 0$ and $\rho = 0.9$ correspond to uncorrelated scenario and highly correlated scenario, respectively. We can find from Fig. 3 that the BER performance of ZF-DCNN detector improves with the increasing of correlation level, which indicates that the DCNN can suppress the influence of correlated noise successfully when the correlation coefficient enlarges. Moreover, the BER performance of ZF-DCNN detector improves with the number of iterations between the ZF detector and the DCNN. Specifically, the ZF-DCNN with $K = 2$ can reduce the detection error of the conventional ZF detector to about 30% at the correlation level of $\rho = 0.8$, which verifies the effectiveness of the proposed generic iterative framework.

Fig. 4 demonstrates the BER performance of the ZF detector and the ZF-DCNN detector where the SNR varies from 0 dB to 30 dB. The correlation coefficient ρ is set to 0.5, which represents a scenario that the noises are moderately correlated. We can find from Fig. 4 that the BER performance gap between the ZF detector and ZF-DCNN detector enlarges along with the SNR. Increasing the iteration between ZF and DCNN can also help improve the BER performance of ZF-DCNN in a wide range of SNR. In particular, the SNR gain of the ZF-DCNN detector over the standard ZF detector is 5 dB at the BER level of 10^{-2} . This indicates that the

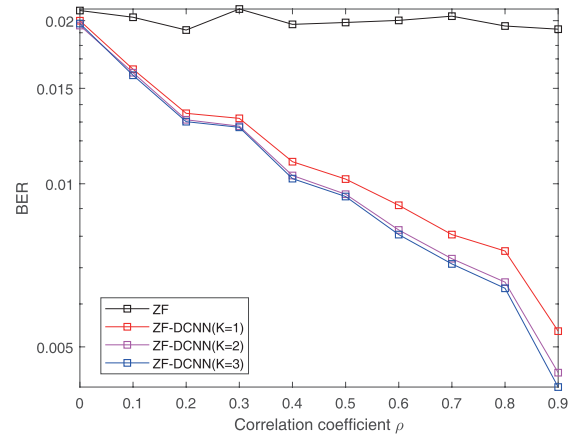


FIGURE 3. BER performance comparison versus correlation coefficient for the ZF detector and ZF-DCNN detector with SNR = 30dB.

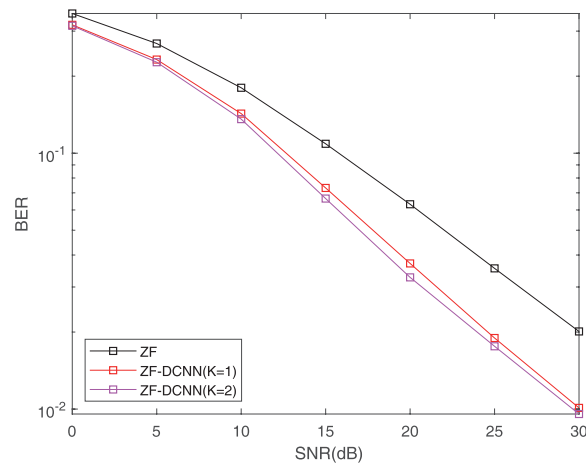


FIGURE 4. BER performance comparison versus SNR for the ZF detector and ZF-DCNN detector with $\rho = 0.5$.

proposed iterative framework outperforms the conventional ZF detector, which further verifies the effectiveness of the proposed generic iterative framework.

In order to validate the generalization of the proposed iterative framework, we also perform some simulations with various linear detectors such as the conventional MMSE, ZF-SIC and MMSE-SIC detectors. Similar to the Fig. 3, Figs. 5-7 demonstrate the BER performance of MMSE and MMSE-DCNN, ZF-SIC and ZF-SIC-DCNN, MMSE-SIC and MMSE-SIC-DCNN in the presence of various correlation levels, respectively. As observed from these figures, all the iterative detectors outperform the corresponding conventional linear detectors in a wide range of correlation coefficient ρ from 0 to 0.9. More specifically, the iterative detectors with $K = 2$ can reduce detection error of the corresponding conventional linear detectors to about 60%, 26% and 30% at the correlation level of $\rho = 0.8$ with respect to MMSE, ZF-SIC and MMSE-SIC, respectively.

Furthermore, as similar with Fig. 4, Figs. 8-10 depict the BER performance of the standard linear detectors as well as

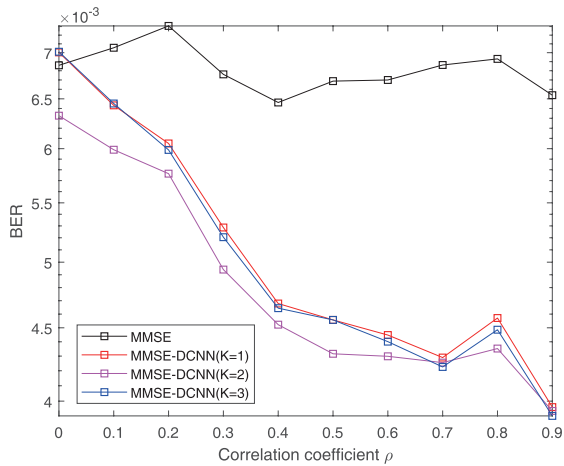


FIGURE 5. BER performance comparison versus correlation coefficient for the MMSE detector and MMSE-DCNN detector with SNR = 30dB.

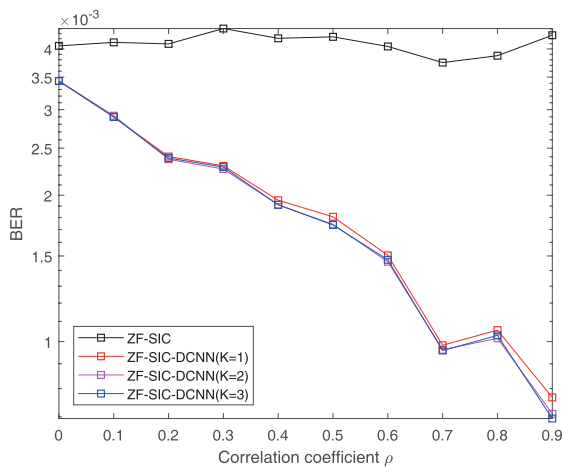


FIGURE 6. BER performance comparison versus correlation coefficient for the ZF-SIC detector and ZF-SIC-DCNN detector with SNR = 30dB.

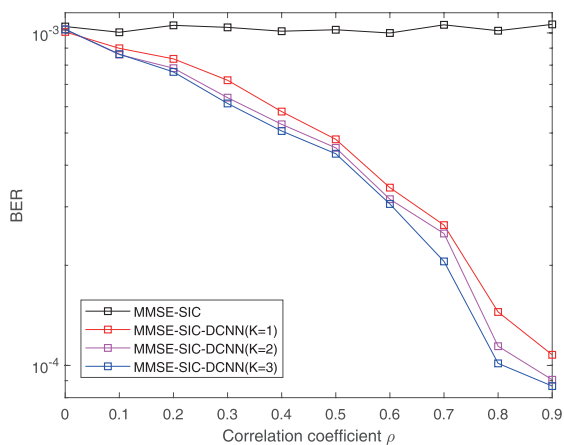


FIGURE 7. BER performance comparison versus correlation coefficient for the MMSE-SIC detector and MMSE-SIC-DCNN detector with SNR = 20dB.

the corresponding iterative detectors in the case that the SNR varies from 0 dB to 30 dB and correlation coefficient $\rho = 0.5$. We can find from these figures that the BER performance gap between the iterative detectors and the corresponding conventional linear detectors enlarges along with the increasing

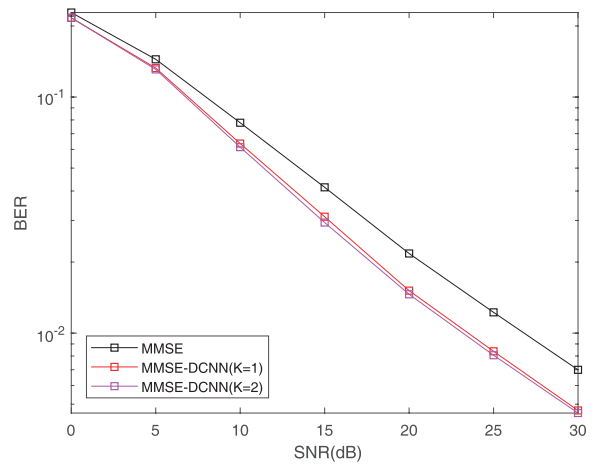


FIGURE 8. BER performance comparison versus SNR for the the MMSE detector and MMSE-DCNN detector with $\rho = 0.5$.

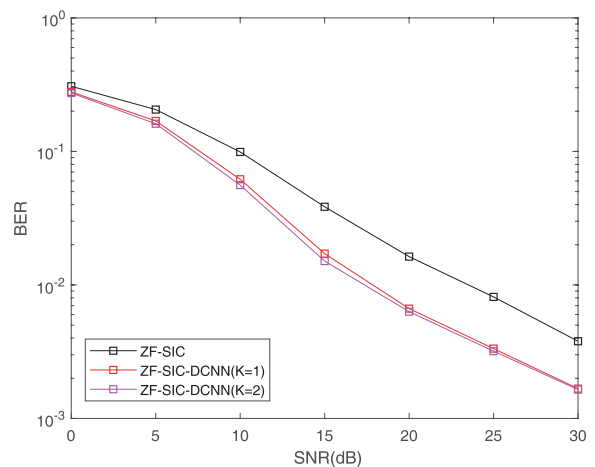


FIGURE 9. BER performance comparison versus SNR for the the ZF-SIC detector and ZF-SIC-DCNN detector with $\rho = 0.5$.

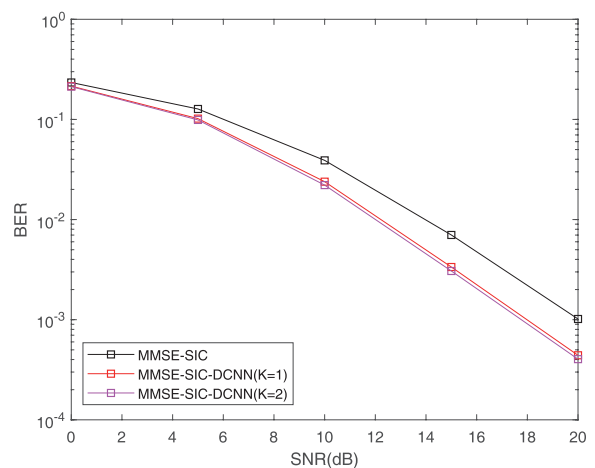


FIGURE 10. BER performance comparison versus SNR for the the MMSE-SIC detector and MMSE-SIC-DCNN detector with $\rho = 0.5$.

SNR. Specifically, the SNR gain of the iterative detectors over the corresponding standard linear detectors is about 5 dB in a wide range of SNRs. This further validates the generalization

of the proposed generic iterative framework in the presence of correlated noise.

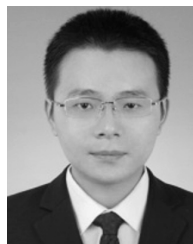
VI. CONCLUSION

In this paper, we employed an iterative framework of DCNN and linear detectors to improve the detection performance for MIMO systems under correlated noise environments, which were effective to support the high data-rate transmission for the wireless communication systems. In this framework, the linear detector such as ZF, MMSE, ZF-SIC and MMSE-SIC produced an initial estimate of transmitted signals, while DCNN output a more accurate estimate of transmitted signals through exploiting the local correlation among noise. Simulation results were demonstrated to show that the proposed detector could outperform the conventional linear detectors substantially. In future works, we will apply this work to IoT applications, such as the urban environments detecting [42]–[46]. Moreover, we will investigate other intelligent algorithms [47]–[51], and apply to the MIMO systems in order to further enhance the detection performance. In further, we will apply the work in this paper into the mobile edge computing [52], [53], and try to enhance the system performance.

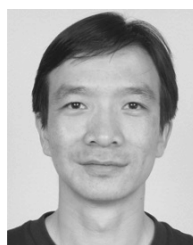
REFERENCES

- [1] F. Shi, J. Xia, Z. Na, X. Liu, Y. Ding, and Z. Wang, "Secure probabilistic caching in random multi-user multi-UAV relay networks," *Phys. Commun.*, vol. 32, pp. 31–40, Feb. 2019.
- [2] L. Fan, N. Zhao, X. Lei, Q. Chen, N. Yang, and G. K. Karagiannidis, "Outage probability and optimal cache placement for multiple amplify-and-forward relay networks," *IEEE Trans. Veh. Technol.*, vol. 67, no. 12, pp. 12373–12378, Dec. 2018.
- [3] X. Lai, W. Zou, D. Xie, X. Li, and L. Fan, "DF relaying networks with randomly distributed interferers," *IEEE Access*, vol. 5, pp. 18909–18917, 2017.
- [4] J. Xia, D. Deng, Y. Rao, D. Li, F. Zhu, and L. Fan, "When distributed switch-and-stay combining meets buffer in IoT relaying networks," *Phys. Commun.*, vol. 38, Feb. 2020, Art. no. 100920.
- [5] C. Li, "Cache-enabled physical-layer secure game against smart UAV-assisted attacks in B5G noma networks," *EURASIP J. Wireless Commun. Netw.*, vol. 2020, p. 7, Dec. 2019.
- [6] J. Xia, "Cache-aided mobile edge computing for B5G wireless communication networks," *EURASIP J. Wireless Commun. Netw.*, vol. 2020, p. 15, Dec. 2020.
- [7] Z. Na, Y. Wang, X. Li, J. Xia, X. Liu, M. Xiong, and W. Lu, "Subcarrier allocation based simultaneous wireless information and power transfer algorithm in 5G cooperative OFDM communication systems," *Phys. Commun.*, vol. 29, pp. 164–170, Aug. 2018.
- [8] X. Lin, J. Xia, and Z. Wang, "Probabilistic caching placement in UAV-assisted heterogeneous wireless networks," *Phys. Commun.*, vol. 33, pp. 54–61, Apr. 2019.
- [9] S. Lai, "Intelligent secure communication for cognitive networks with multiple primary transmit power," *IEEE Access*, to be published.
- [10] X. Lai, L. Fan, X. Lei, J. Li, N. Yang, and G. K. Karagiannidis, "Distributed secure switch-and-stay combining over correlated fading channels," *IEEE Trans. Inf. Forensics Security*, vol. 14, no. 8, pp. 2088–2101, Aug. 2019.
- [11] C. Li, W. Zhou, K. Yu, L. Fan, and J. Xia, "Enhanced secure transmission against intelligent attacks," *IEEE Access*, vol. 7, pp. 53596–53602, 2019.
- [12] J. Yang, D. Ruan, J. Huang, X. Kang, and Y.-Q. Shi, "An embedding cost learning framework using GAN," *IEEE Trans. Inf. Forensics Security*, vol. 15, pp. 839–851, 2020.
- [13] Z. Na, J. Lv, M. Zhang, B. Peng, M. Xiong, and M. Guan, "GFDM based wireless powered communication for cooperative relay system," *IEEE Access*, vol. 7, pp. 50971–50979, 2019.
- [14] J. Xia, L. Fan, W. Xu, X. Lei, X. Chen, G. K. Karagiannidis, and A. Nallanathan, "Secure cache-aided multi-relay networks in the presence of multiple eavesdroppers," *IEEE Trans. Commun.*, vol. 67, no. 11, pp. 7672–7685, Nov. 2019.
- [15] J. Zhao, X. Guan, and X. P. Li, "Power allocation based on genetic simulated annealing algorithm in cognitive radio networks," *Chin. J. Electron.*, vol. 22, no. 1, pp. 177–180, Jan. 2013.
- [16] J. Zhao, S. Ni, L. Yang, Z. Zhang, Y. Gong, and X. You, "Multiband cooperation for 5G HetNets: A promising network paradigm," *IEEE Veh. Technol. Mag.*, vol. 14, no. 4, pp. 85–93, Dec. 2019.
- [17] B. Wang, F. Gao, S. Jin, H. Lin, and G. Y. Li, "Spatial- and frequency-wideband effects in millimeter-wave massive MIMO systems," *IEEE Trans. Signal Process.*, vol. 66, no. 13, pp. 3393–3406, Jul. 2018.
- [18] H. Xie, F. Gao, S. Zhang, and S. Jin, "A unified transmission strategy for TDD/FDD massive MIMO systems with spatial basis expansion model," *IEEE Trans. Veh. Technol.*, vol. 66, no. 4, pp. 3170–3184, Apr. 2017.
- [19] X. Hu, C. Zhong, X. Chen, W. Xu, and Z. Zhang, "Cluster grouping and power control for angle-domain MmWave MIMO NOMA systems," *IEEE J. Sel. Topics Signal Process.*, vol. 13, no. 5, pp. 1167–1180, Sep. 2019.
- [20] W. Xu, J. Liu, S. Jin, and X. Dong, "Spectral and energy efficiency of multi-pair massive MIMO relay network with hybrid processing," *IEEE Trans. Commun.*, vol. 65, no. 9, pp. 3794–3809, Sep. 2017.
- [21] C. Lu, W. Xu, S. Jin, and K. Wang, "Bit-level optimized neural network for multi-antenna channel quantization," *IEEE Wireless Commun. Lett.*, vol. 9, no. 1, pp. 87–90, Jan. 2020.
- [22] Z. Junhui, Y. Tao, G. Yi, W. Jiao, and F. Lei, "Power control algorithm of cognitive radio based on non-cooperative game theory," *China Commun.*, vol. 10, no. 11, pp. 143–154, Nov. 2013.
- [23] J. Zhao, Q. Li, Y. Gong, and K. Zhang, "Computation offloading and resource allocation for cloud assisted mobile edge computing in vehicular networks," *IEEE Trans. Veh. Technol.*, vol. 68, no. 8, pp. 7944–7956, Aug. 2019.
- [24] S. Ni, J. Zhao, H. H. Yang, and Y. Gong, "Enhancing downlink transmission in MIMO HetNet with wireless backhaul," *IEEE Trans. Veh. Technol.*, vol. 68, no. 7, pp. 6817–6832, Jul. 2019.
- [25] C. Li, Y. Xu, J. Xia, and J. Zhao, "Protecting secure communication under UAV smart attack with imperfect channel estimation," *IEEE Access*, vol. 6, pp. 76395–76401, 2018.
- [26] Y. Xu, J. Xia, H. Wu, and L. Fan, "Q-learning based physical-layer secure game against multiagent attacks," *IEEE Access*, vol. 7, pp. 49212–49222, 2019.
- [27] X. Lin, Y. Tang, X. Lei, J. Xia, Q. Zhou, H. Wu, and L. Fan, "MARL-based distributed cache placement for wireless networks," *IEEE Access*, vol. 7, pp. 62606–62615, 2019.
- [28] G. Gui, H. Huang, Y. Song, and H. Sari, "Deep learning for an effective nonorthogonal multiple access scheme," *IEEE Trans. Veh. Technol.*, vol. 67, no. 9, pp. 8440–8450, Sep. 2018.
- [29] Y. Wang, M. Liu, J. Yang, and G. Gui, "Data-driven deep learning for automatic modulation recognition in cognitive radios," *IEEE Trans. Veh. Technol.*, vol. 68, no. 4, pp. 4074–4077, Apr. 2019.
- [30] H. Huang, Y. Peng, J. Yang, W. Xia, and G. Gui, "Fast beamforming design via deep learning," *IEEE Trans. Veh. Technol.*, vol. 69, no. 1, pp. 1065–1069, Jan. 2020.
- [31] K. He, "A MIMO detector with deep learning in the presence of correlated interference," *IEEE Trans. Veh. Technol.*, to be published.
- [32] B. Lu, "Interference suppression by exploiting wireless cache in relaying networks for B5G communications," *Phys. Commun.*, to be published.
- [33] D. Deng, "Link selection in buffer-aided cooperative networks for green IoT," *IEEE Access*, to be published.
- [34] W. Huang, "Multi-antenna processing based cache-aided relaying networks for B5G communications," *Phys. Commun.*, to be published.
- [35] X. Wang, "Joint resource allocation for cognitive OFDM-NOMA systems with energy harvesting in green IoT," *IEEE Access*, to be published.
- [36] K. He, "Ultra-reliable MU-MIMO detector based on deep learning for 5G/B5G-enabled IoT," *EURASIP J. Wireless Commun. Netw.*, to be published.
- [37] K. Zhang, W. Zuo, Y. Chen, D. Meng, and L. Zhang, "Beyond a Gaussian Denoiser: Residual learning of deep CNN for image denoising," 2016, *arXiv:1608.03981*. [Online]. Available: <http://arxiv.org/abs/1608.03981>
- [38] V. Nair and G. E. Hinton, "Rectified linear units improve restricted Boltzmann machines," in *Proc. 27th Int. Conf. Mach. Learn. (ICML)*, 2010, pp. 807–814.
- [39] M. Li, T. Zhang, Y. Chen, and A. J. Smola, "Efficient mini-batch training for stochastic optimization," in *Proc. 20th ACM SIGKDD Int. Conf. Knowl. Discovery Data Mining (KDD)*, 2014, pp. 661–670.

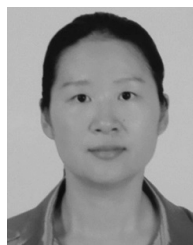
- [40] K. He and J. Sun, "Convolutional neural networks at constrained time cost," in *Proc. IEEE Conf. Comput. Vis. Pattern Recognit. (CVPR)*, Jun. 2015, pp. 5353–5360.
- [41] M. K. Simon and M. S. Alouini, *Digital Communication over Fading Channels*, 2nd ed. Hoboken, NJ, USA: Wiley, 2005.
- [42] J. Yang, Z. Lin, H. Wu, Q. Chen, X. Xu, G. Huang, L. Fan, X. Shen, and K. Gan, "Inverse optimization of building thermal resistance and capacitance for minimizing air conditioning loads," *Renew. Energy*, vol. 148, pp. 975–986, Apr. 2020.
- [43] C. Fan and Y. Ding, "Cooling load prediction and optimal operation of HVAC systems using a multiple nonlinear regression model," *Energy Buildings*, vol. 197, pp. 7–17, Aug. 2019.
- [44] J. Yang, H. Wu, X. Xu, G. Huang, T. Xu, S. Guo, and Y. Liang, "Numerical and experimental study on the thermal performance of aerogel insulating panels for building energy efficiency," *Renew. Energy*, vol. 138, pp. 445–457, Aug. 2019.
- [45] C. Fan, Y. Ding, and Y. Liao, "Analysis of hourly cooling load prediction accuracy with data-mining approaches on different training time scales," *Sustain. Cities Soc.*, vol. 51, Nov. 2019, Art. no. 101717.
- [46] H. Huang, Y. Zhou, R. Huang, H. Wu, Y. Sun, G. Huang, and T. Xu, "Optimum insulation thicknesses and energy conservation of building thermal insulation materials in Chinese zone of humid subtropical climate," *Sustain. Cities Soc.*, vol. 52, Jan. 2020, Art. no. 101840.
- [47] G. Liu, Y. Xu, Z. He, Y. Rao, J. Xia, and L. Fan, "Deep learning-based channel prediction for edge computing networks toward intelligent connected vehicles," *IEEE Access*, vol. 7, pp. 114487–114495, 2019.
- [48] Z. Zhao, R. Zhao, J. Xia, X. Lei, D. Li, C. Yuen, and L. Fan, "A novel framework of three-hierarchical offloading optimization for MEC in industrial IoT networks," *IEEE Trans. Ind. Informat.*, to be published.
- [49] M.-S. Baek, S. Kwak, J.-Y. Jung, H. M. Kim, and D.-J. Choi, "Implementation methodologies of deep learning-based signal detection for conventional MIMO transmitters," *IEEE Trans. Broadcast.*, vol. 65, no. 3, pp. 636–642, Sep. 2019.
- [50] J. Xia, Y. Xu, D. Deng, Q. Zhou, and L. Fan, "Intelligent secure communication for Internet of Things with statistical channel state information of attacker," *IEEE Access*, vol. 7, pp. 144481–144488, 2019.
- [51] Y. Guo, Z. Zhao, R. Zhao, S. Lai, Z. Dan, J. Xia, and L. Fan, "Intelligent offloading strategy design for relaying mobile edge computing networks," *IEEE Access*, to be published.
- [52] R. Zhao, "Deep reinforcement learning based mobile edge computing for intelligent Internet of Things," *IEEE Access*, to be published.
- [53] Z. Zhao, "Intelligent mobile edge computing with pricing in Internet of Things," *IEEE Access*, to be published.



WEI HUANG received the bachelor's degree from the Department of Computer Science, Hubei Minzu University, in 2010, and the master's degree from the Department of Mechanical Electronic Engineering, Donghua University, in 2014. He is currently a Research Assistant with the School of Computer Science, Guangzhou University. His research interests include intelligent accumulator design and deep-learning in edge computing, and the Internet of Things.



DAN DENG received the bachelor's and Ph.D. degrees from the Department of Electronic Engineering and Information Science, University of Science and Technology of China, in 2003 and 2008, respectively. From 2008 to 2014, he was with Comba Telecom Ltd., Guangzhou, China, as the Director. Since 2014, he has been with Guangzhou Panyu Polytechnic, where he is currently an Associate Professor. He has published 45 articles in international journals and conferences, and holds 19 patents. His research interests include MIMO communication and physical-layer security in next-generation wireless communication systems. He has served as a member for technical program committees for several conferences.



JUNJUAN XIA received the bachelor's degree from the Department of Computer Science, Tianjin University, in 2003, and the master's degree from the Department of Electronic Engineering, Shantou University, in 2015. She is currently working with the School of Computer Science and Cyber Engineering, Guangzhou University, as a Laboratory Assistant. Her current research interests include wireless caching, physical-layer security, cooperative relaying, and interference modeling.



LISENG FAN received the Ph.D. degree from the Tokyo Institute of Technology, Tokyo, in 2008. He is currently a Professor with the School of Computer Science and Cyber Engineering, Guangzhou University. He has published more than 40 articles in the IEEE journals and conferences. His main research interests include the information security, wireless networks, and the artificial intelligence. His recent research interests are in the application of artificial intelligence into the wireless networks.



KE HE received the bachelor's degree in software engineering from the Wuhan University of Technology, in 2015. He is currently pursuing the master's degree with the School of Computer Science, Guangzhou University. His current research interests focus on statistical machine learning and artificial intelligence.



ZIZHI WANG received the bachelor's degree in software engineering from Xinjiang University, in 2019. He is currently pursuing the master's degree with the School of Computer Science, Guangzhou University. His research interests focus on deep-learning in signal detection and estimation.